

RESEARCH ARTICLE

Spatial migration and distribution of suspended particles in saturated sand layer under the impact of temperature

Xianze Cui^{1,2,3} | Jin Li^{1,2} | Guangdong Yang^{1,2} | Wenbin Fei⁴ | Shengyong Ding^{1,2} | Yong Fan^{1,2}

¹Hubei Key Laboratory of Construction and Management in Hydropower Engineering, China Three Gorges University, Yichang, China

²College of Hydraulic & Environmental Engineering, China Three Gorges University, Yichang, China

³MOE Key Laboratory of Groundwater Circulation and Environmental Evolution, China University of Geosciences (Beijing), Beijing, People's Republic of China

⁴Department of Infrastructure Engineering, The University of Melbourne, Parkville, Australia

Correspondence

Yong Fan, Hubei Key Laboratory of Construction and Management in Hydropower Engineering, China Three Gorges University, No. 8, University Road, Yichang 443002, People's Republic of China.

Email: yfan@ctgu.edu.cn

Funding information

Educational Commission of Hubei Province of China, Grant/Award Number: T2020005; National Natural Science Foundation of China, Grant/Award Number: 41702254; Natural Science Foundation of Hubei Province, Grant/Award Number: 2022CFB248; Research Project of Hubei Provincial Department of Education, Grant/Award Number: B2021037; The Young Top-notch Talent Cultivation Program of Hubei Province

Abstract

The migration, deposition and detachment of suspended particles in saturated sands are used in many fields. Temperature is an important influencing factor in the transport and deposition process of particles in porous media, and it plays an important role in ground-water heat pump (GWHP) projects. This article discusses the independent development of a three-dimensional percolation sandbox test device and the design of a particle migration test based on the Reynolds number in the context of the backfilling process of GWHP systems as the experimental background. The effects of various temperatures (10, 25, and 40°C) on the movement of suspended particles in porous media were studied. The experimental results showed that as the temperature rose, more particles were deposited in the sand layer, the uneven flow of particles in the sand layer accelerated, and the particles spread out in the direction opposite to the non-percolation direction with a wider distribution range in the sandbox. Increased temperature also promoted the percolation of smaller particles, causing the diffusion zone to terminate sooner and the deposition zone to last longer, resulting in the capture of more particles on the surface and in the pore channels of the sand layer.

KEY WORDS

groundwater heat pump, natural sand, particle migration, temperature, three-dimensional sand box

1 | INTRODUCTION

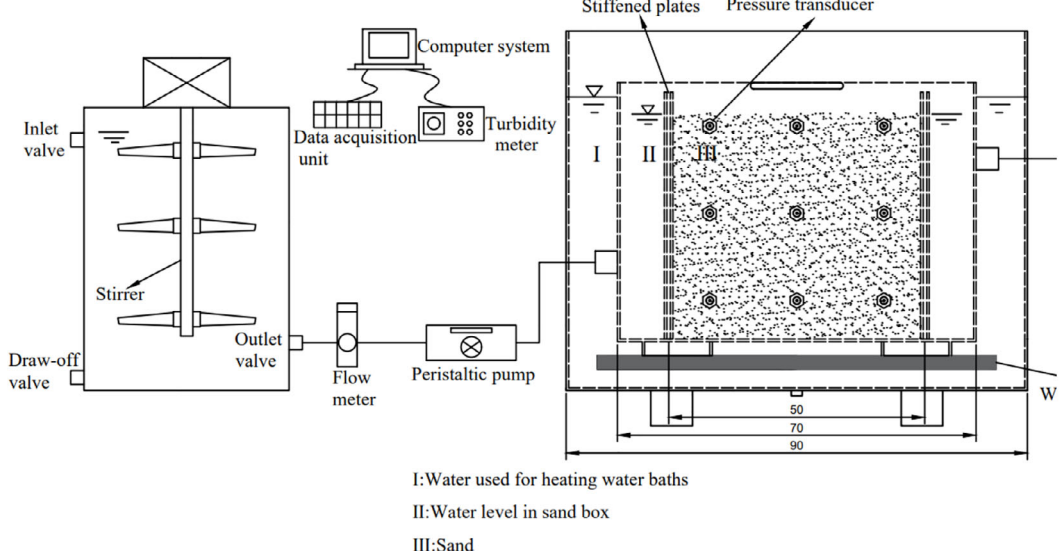
Applications in various fields, such as wastewater treatment (Gjengedal et al., 2020; Shabani et al., 2019), groundwater replenishment (Pan et al., 2021), treatment of heavy metal contamination, biofilm bacterial purification (Seifert & Engesgaard, 2012), and processing of nuclear waste, exploit the migration, deposition, and detachment of suspended particles in saturated sand layers. Temperature has a significant influence on the transport and deposition of particles in porous media, and it is also a significant factor in projects involving heat pumps for groundwater as sources of heat (Blum et al., 2011; Sarbu & Sebarchievici, 2014).

For example, a system for using groundwater as a low-level heat source depends upon heat pump technology to transfer cold and hot fluids from low-level to high-level energy using only a tiny amount of electrical energy (Ahmadi et al., 2018). It is necessary to replenish these systems to safeguard groundwater resources and maintain a steady groundwater level. Groundwater recharge, however, is often difficult and challenging in practice (Cui, Fan, & Wang, 2019; Cui, Fan, Wang, & Huang, 2019; Dallmann et al., 2020; García-Gil et al., 2016). Interactions between porous media, groundwater, and recharge water during the recharge process damage the pore structure of aquifers and obstruct systems (Tao et al., 2019). The permeability of an aquifer

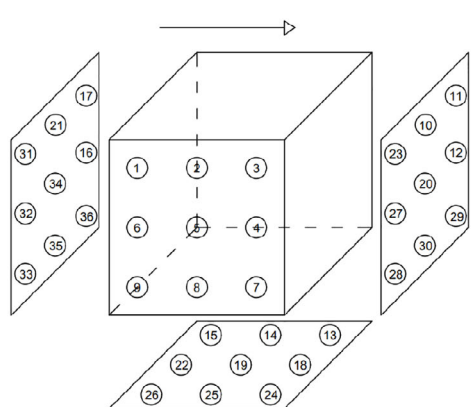
gradually diminishes at the well wall, in the gravel-filled area, and near the well wall as blockages accumulate over time (Liu et al., 2015). The development of blockages in an aquifer is related to many factors, such as the quality of the recharge water, physical properties of the aquifer, and chemical environment, and they can be classified as physical, bubble, chemical, and biological blockages (Lumbangaol et al., 2021; Mauclaire et al., 2006). The most prevalent are physical blockages, which account for more than 60% of clogs caused by recharging.

Most current studies on the migration characteristics of suspended particles in porous media focus on physical, chemical, and biological processes, in particular, the effects of particle size (Cui, Fan, & Wang, 2019; Cui, Fan, Wang, & Huang, 2019; Shaniv et al., 2021), flow rate (Ahfir et al., 2007; Alem et al., 2013; Sasidharan et al., 2014; Won et al., 2020), chemical environment (Mek et al., 2020), heavy metal ions (Bai et al., 2020; Nie et al., 2021), and microbial microplastics (Chrysikopoulos & Aravantinou, 2014; Dong et al., 2021; Jiang et al., 2021; Kim & Walker, 2009; Lumbangaol et al., 2021; Wang et al., 2022) at room temperature. Temperature is another very

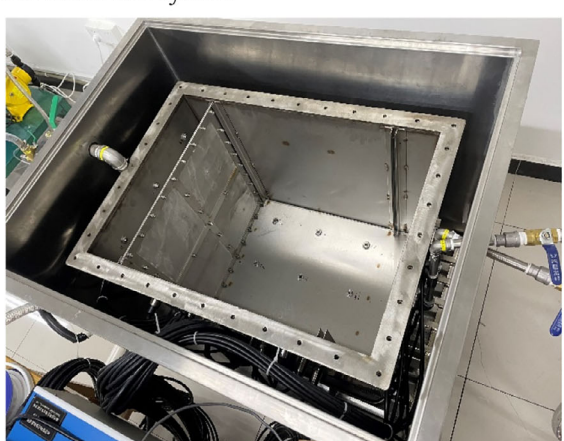
essential consideration for heat pump systems for groundwater. It has been reported that temperature fluctuations have a substantial impact on the movement, deposition, and aggregation of contaminated particles in recharge water in pore channels. The permeability coefficient of sandstone aquifers containing the clay mineral kaolinite dramatically decreases as the temperature rises (Rosenbrand et al., 2014). Temperature increases the stability of bentonite colloids (Sasidharan et al., 2014). Temperature has an impact on the forces acting on particles, and it has a larger effect on electrostatic forces and a smaller effect on water viscosity (You et al., 2015). Researchers discovered that increasing the temperature enhances the migration of particles (e.g., copper ions, graphene oxide particles, and silica powders [Bai et al., 2021]) in porous media while lowering the particle transport velocity (Bai et al., 2016; Bing et al., 2021). If there is a temperature differential between a porous medium and an incoming fluid, then particle deposition in the porous medium increases as the temperature difference grows (Li et al., 2016). Temperature, in combination with other parameters, affects the migratory properties of particles in porous media. Repulsion between suspended particles dominates at



(a) Schematic diagram of the test system



(b) Pressure monitoring tube location



(c) Real picture of sand box

FIGURE 1 Test system and detail diagram.

pH = 7 and $T \leq 30^{\circ}\text{C}$, while Brownian motion dominates at $T > 30^{\circ}\text{C}$ (Xue et al., 2019). The temperature effect is greatly diminished when the percolation velocity and particle size are both minimal (Cui, Fan, & Wang, 2019; Cui, Fan, Wang, & Huang, 2019).

Many scholars have studied the migration and deposition of suspended particles in saturated porous media, but the majority of studies on the effect of temperature on the particle transport process use one-dimensional sand column tests, and few use three-dimensional sandbox conditions, which are more realistic. In this study, a three-dimensional percolation sandbox test system was developed in this laboratory and used to investigate the effect of temperature on the movement of suspended particles in porous media. This system was used to measure indicators such as percolation velocity, pressure variation, flow rate, and particle concentration, and it could operate for a long time under constant temperature and pressure settings.

2 | EXPERIMENTAL OVERVIEWS

2.1 | Experimental equipment

The recharge process of the ground water heat pump (GWHP) system was studied, and the particle migration test was designed based on the Reynolds number. A sandbox was used to simulate an aquifer near a recharge well, and the test setup is shown in Figure 1a. The system mainly included a three-dimensional sand column test box, inlet tank, outlet tank, flow meter, turbidity meter, water pump, metallographic microscope and particle size analyser. The system was used to measure indicators such as seepage velocity, pressure change, flow rate, and particle concentration before and after a liquid passed through the sand in the test box, and it could maintain long operation under constant temperature, pressure and other conditions. The temperature of the groundwater that was available for the heat pump was from 12 to 22°C in winter and from 18 to 35°C in summer. Three temperatures, 10, 25, and 40°C , were selected as the test temperatures. The outer layer of the sandbox was a temperature-controlled water tank that was connected to an electric heater. The temperature of the test sandbox was adjusted through water circulation. The inner layer of the sandbox was a test sandbox that was 500 mm × 500 mm × 500 mm, and both ends of the inner sandbox were equipped with movable baffles that resisted pressure. The baffle mesh was adjusted according to the test requirements. The inner sandbox was equipped with 36 sensor interfaces on 4 sides, and they were connected to an external data collector. The position of the pressure sensor is shown in Figure 1b. The inlet tank was equipped with a large agitator to ensure uniform distribution of particles inside the tank.

2.2 | Experimental materials

In recent years, the clogging of layers by particles during recharge has been a major problem in sandstone aquifers. To more realistically simulate the engineering conditions, washed natural sand (light yellow in

colour with stable chemical properties, hard texture and good wear resistance) was selected as the filling material in the test sandbox. White silica micropowder was used as the suspended particle material in the test; it was nearly spherical in shape with stable physical and chemical properties, and easy to observe after sampling. According to engineering data and experience from a previous study, In the groundwater source heat pump and other projects, the particles that trigger the recharge blockage are mainly concentrated above 10 μm , while the sand of 1000–2000 μm is selected for the test according to the particle size of the porous media of the stratum. And the particle size and the gradation curve of the selected material are shown in Figure 2 and Table 1, and the roundness of the white fumed silica is shown in Figure 3.

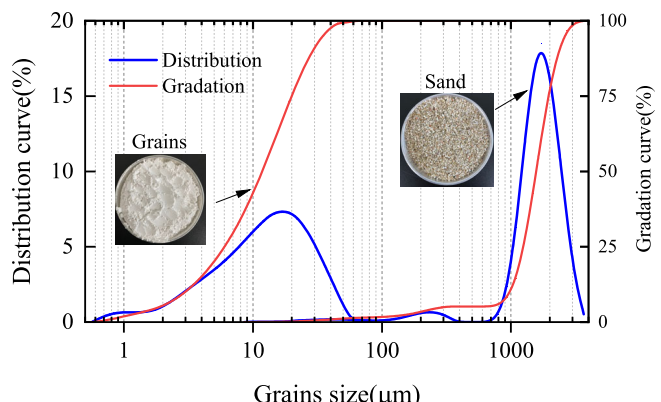


FIGURE 2 Grading curves of natural sand and silica micronaire.

TABLE 1 Test material parameters.

Material	Particle size (μm)	Median particle size (μm)	Porosity (%)	Specific surface area (m^2/kg)
Sand	1000–2000	1568	42	8
Grains	6–17	12	-	772

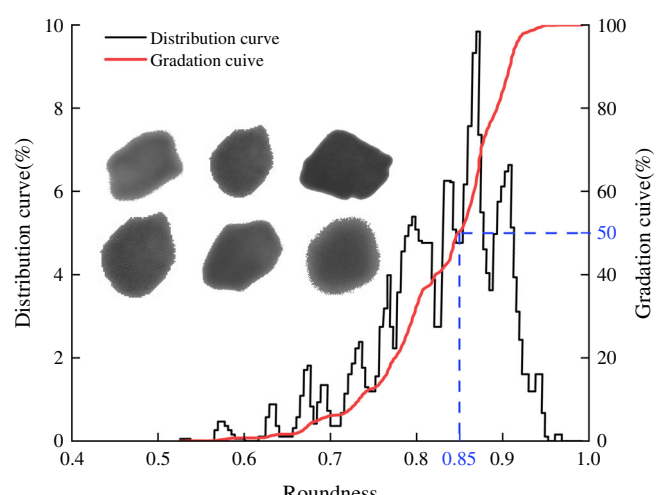


FIGURE 3 Roundness of grains.

2.3 | Experimental process

The water temperature available for the groundwater source heat pump unit is 12–22°C in winter, while the water temperature is 18–35°C in summer, and three temperatures of 10, 25, and 40°C were selected as the test temperatures. The test flow rate was selected as the test flow rate of 0.01 cm/s (flow rate in the sand box) based on the authors' previous related simulations (Cui, Fan, & Wang, 2019; Cui, Fan, Wang, & Huang, 2019), where the seepage velocity between

different recharge wells was around 0.01 cm/s, and the flow rate was 95 L/h. And the volume of the inlet tank was 600 L. The main test process was divided into the following steps.

1. Before the test, the natural sand was repeatedly cleaned to remove suspended impurities and placed into an oven at 105°C for 24 h. The washed natural sand was used to fill the sandbox by the layered wet filling method. The water surface of each layer has higher than the upper surface of the sand layer by ~1 cm to

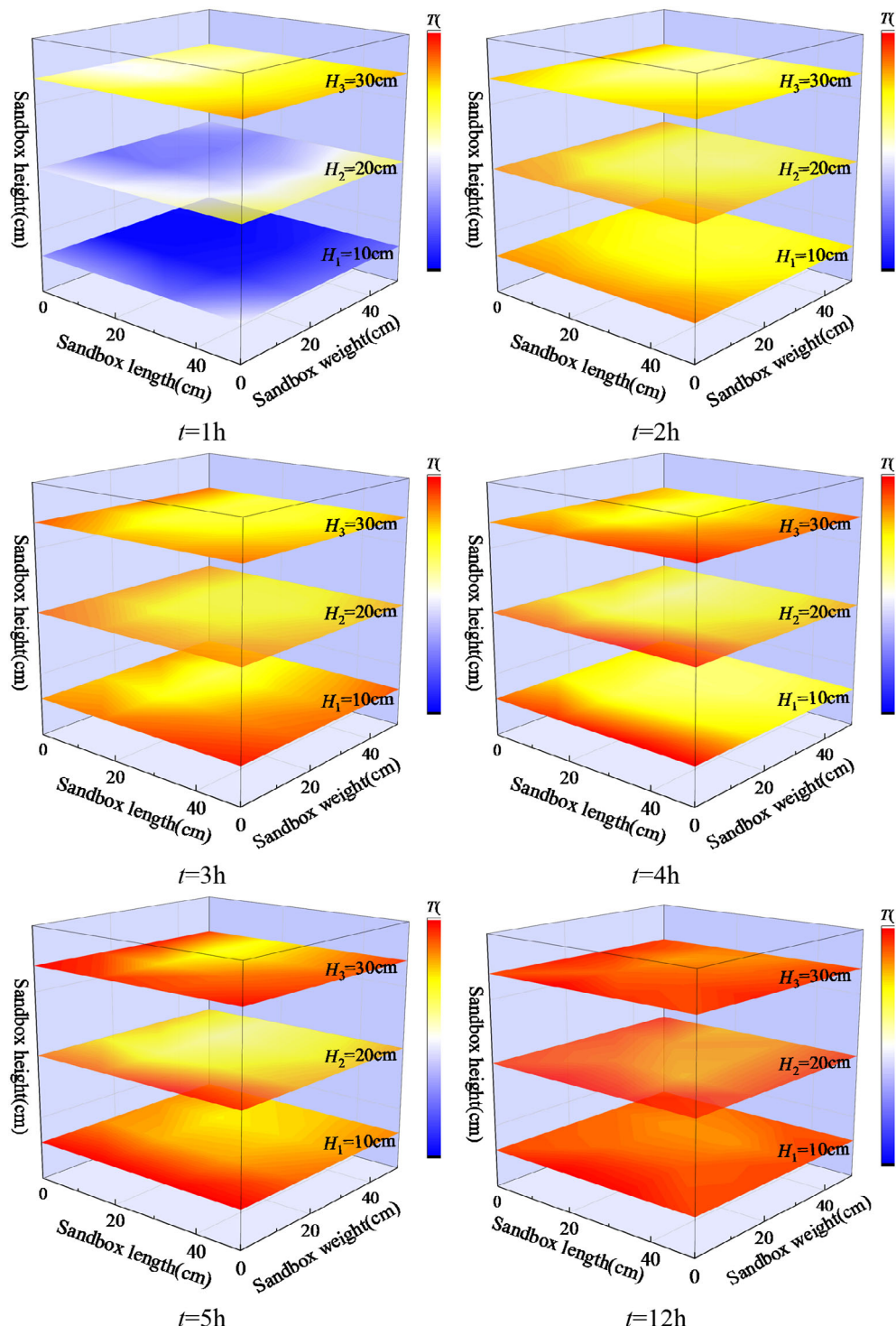


FIGURE 4 Variation of temperature with heating time at different points in step 2, t is the heating time, H is the sand layer height.

ensure that the filled specimen was saturated. The sand layer was properly pounded and compacted to ensure the uniformity of the sand layer when filling in layers. Here in four layers of filling, a total of 40 cm high filling.

2. The outer temperature-controlled water tank was opened, the sandbox was heated to the specified temperature, and the temperature was monitored at all times during the heating process. The

sandbox was divided into three layers (H1, H2, H3) that were 10, 20 and 30 cm from the bottom of the sandbox. There were 16 points for monitoring temperature in each layer and 48 points in total, as shown in Figure 4 (40°C test as an example).

3. The water pump was turned on, and clear water was passed through the sand until the turbidity of the effluent was nephelometric turbidity unit (NTU) <2. Then, the water pump was turned off, the remaining clear water in the tank was removed, and 0.5 g/L of a suspension of micronized silica (turbidity 170 NTU) was added. The pump was turned on, and the suspension was injected in the process of opening the stirrer so that it was distributed uniformly through the sand, and the test began.
4. Each group of tests was conducted for 72 h while the pressure in the sand tank was monitored in real time every 10 s by 36 pressure sensors. Every 30 min, a sample of liquid was collected from the outlet to measure its turbidity. When almost all the suspension in the tank was used, more suspension at the same concentration, which had been prepared in advance, was added.
5. After the test, the remaining water in the sandbox was slowly removed, and the mass percentage of sand and particles at each point and the particle size distribution of the particles that formed a blockage in the sandbox were measured. The mass percentage showed the deposition and clogging by particles at the point positions, and Figure 5 shows a map of the point positions.

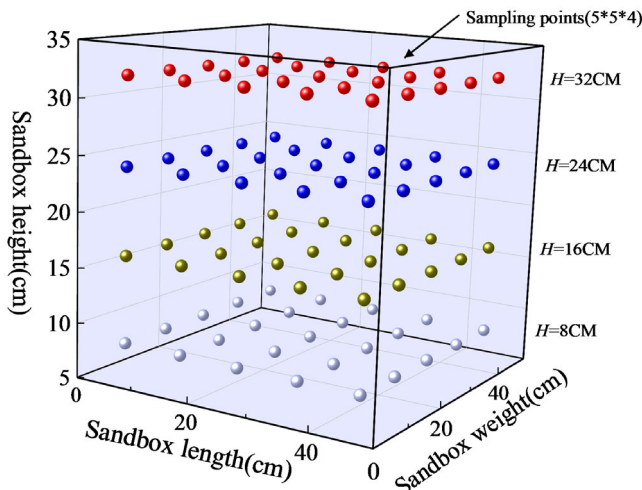


FIGURE 5 Spatial distribution map of sampling points in step 5.

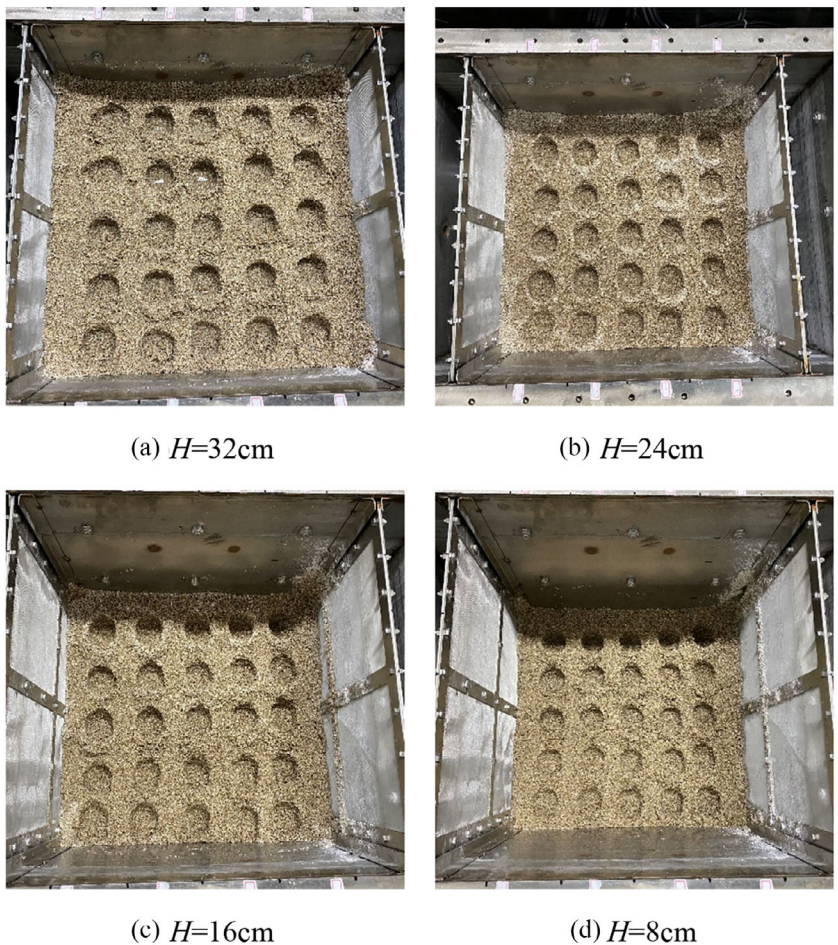


FIGURE 6 Pictures of the point sampling in step 5 at the end of the test, H is the sand layer height.

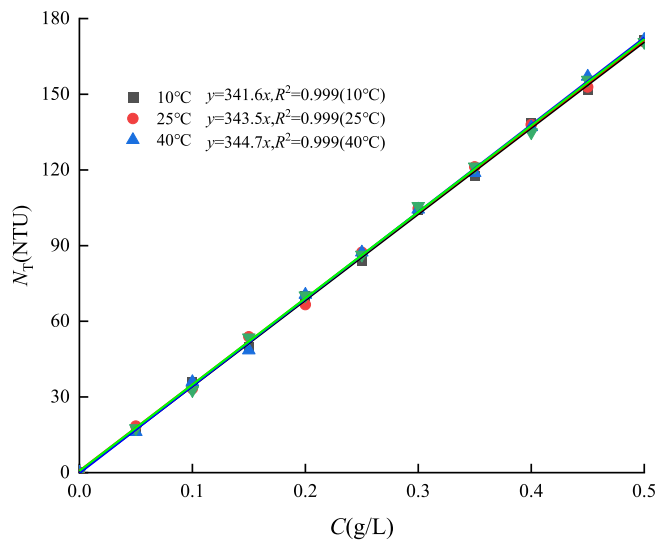


FIGURE 7 The relationship curve between particle turbidity and concentration.

6. Samples were taken from the points where clogging was obvious, dried, and observed under a microscope.

3 | ANALYSIS OF TEST RESULTS

3.1 | Amount of particle deposition

Figure 6 shows the sampling plot for each layer of points. The mass percentage R of sand to particles at each point measured to some extent the number of particles deposited at that point; when the value of R was larger, more particles were deposited, and when the value of R was smaller, fewer particles were deposited. Samples were removed at each point with an aluminium box and weighed, and the particles in the box were washed into a small beaker (with a filter pad above the beaker) with water at a fixed level of 200 mL at a time, followed by particle turbidity measurement with a particle size analyser. Many

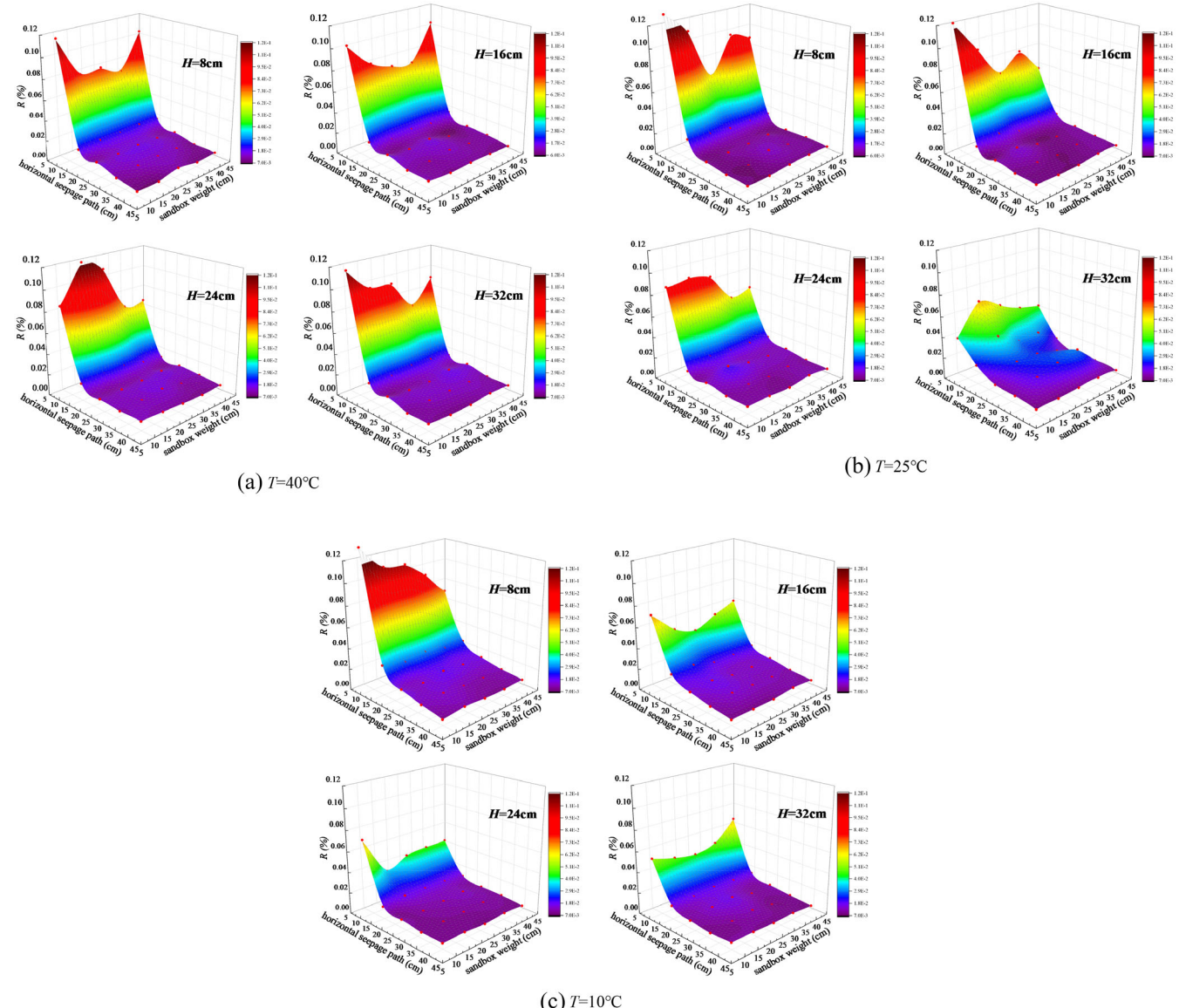
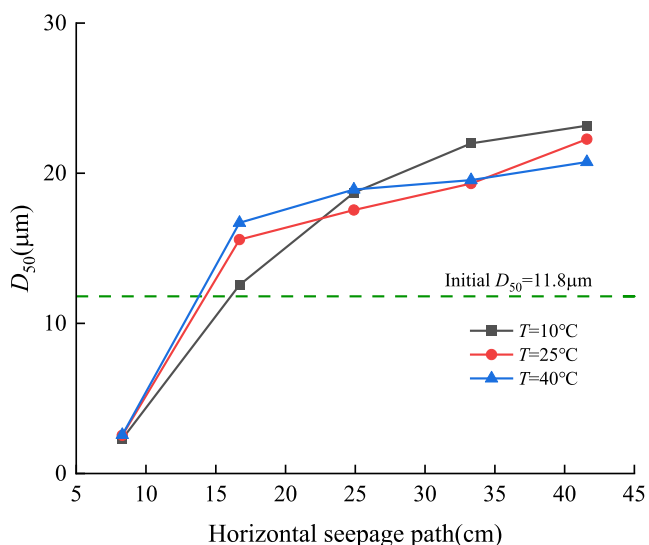
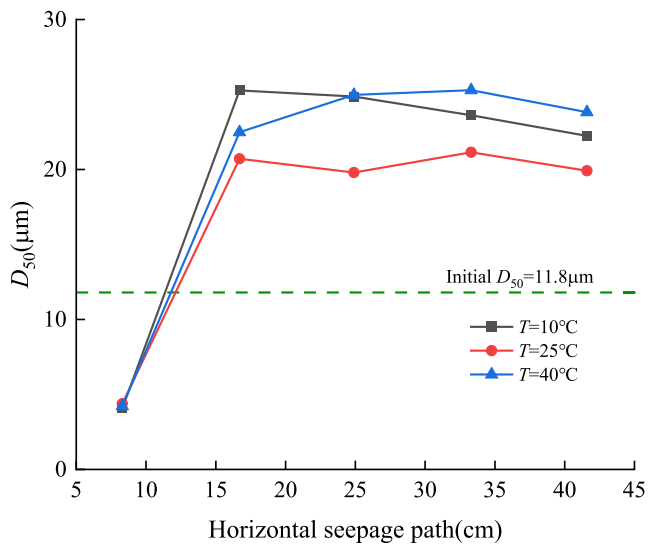


FIGURE 8 Particle deposition at different points of the sandbox at three test temperatures, H is the height (i.e., the distance from the bottom of the sandbox).

studies (Bennacer et al., 2013) pointed out that there is a strong correlation between the concentration of suspended particles and turbidity. A turbidimeter was used to measure the turbidity and then subsequently converted to the concentration of particles. According to the authors, they previously measured the concentration-turbidity relationship. The test used a 0.5 g/mL particle suspension with a turbidity of 170, and there was a linear relationship between turbidity and concentration. The specific relationship between concentration and turbidity is shown in Figure 7. The mass percentages of sand and particles at each point were expressed as R:

$$\begin{cases} R = \frac{m_3}{m_4} \times 100\% \\ m_3 = F(N_T) \\ m_2 = (m - m_1) \times \varphi \\ m_4 = m - m_1 - m_2 - m_3 \end{cases} \quad (1)$$

(a) $H=8\text{cm}$ (c) $H=24\text{cm}$

where m is the mass of the sample (g); m_1 is the mass of the aluminum box (g); m_2 is the mass of water in the sample (g); m_3 is the mass of the particles (g); m_4 is the mass of sand (g); N_T is the measured turbidity of the particles (NTU); the mass of the particles can be converted from the measured turbidity, and the relationship between them is expressed by $F(N_T)$; and φ is the water content.

The results for R at each point are shown in Figure 8a-c. The test results show that the deposition of particles along the percolation direction decreases under different test temperature conditions. The maximum deposition of particles is at 8.3 cm from the inlet, indicating that blockage occurs there, and the deposition of particles decreases the most between the percolation distances of $x = 8.3$ cm and $x = 16.6$ cm, followed by a slow decrease in the deposition of particles. It is obvious from the figure that temperature can affect the deposition of particles. At the maximum test temperature, that is,

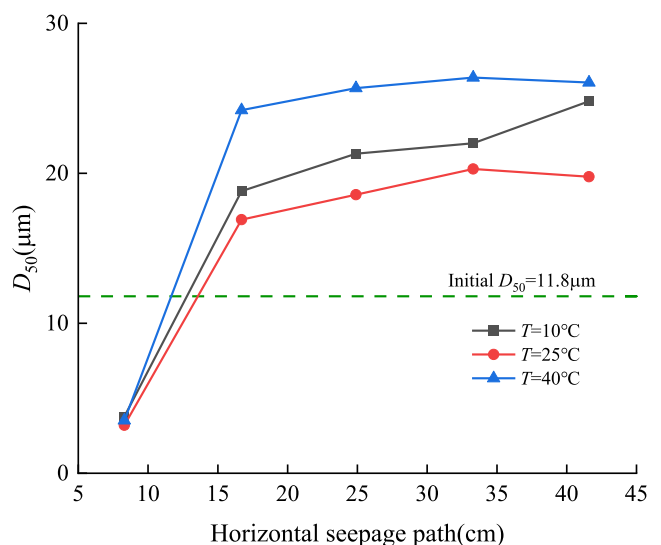
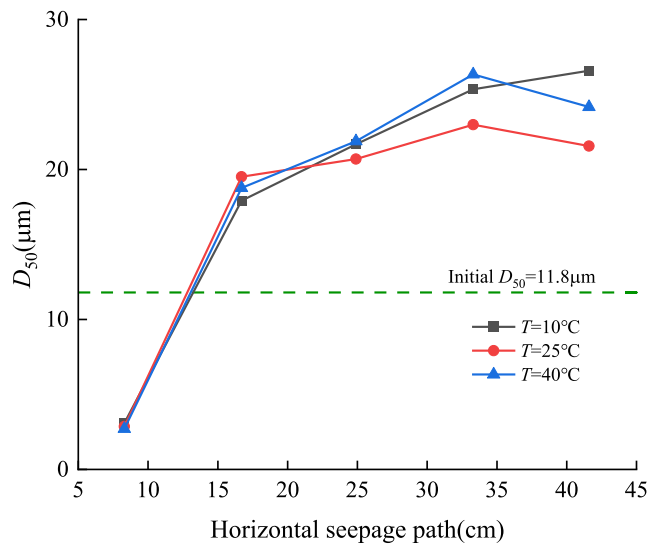
(b) $H=16\text{cm}$ (d) $H=32\text{cm}$

FIGURE 9 Median particle size variation of deposited particles along the seepage distance.

Figure 8a, a number of particles were deposited at all four heights, with R_{\max} values of 0.119%, 0.117%, 0.105%, and 0.117% at 8.3 cm from the water inlet. At the minimum test temperature, that is, Figure 8c, the same indicators were 0.118%, 0.072%, 0.071%, and 0.067%. These results indicate that the higher the temperature is, the wider the location in the longitudinal direction where the deposition of particles occurs. In addition, the migration of particles in the sand-box spreads to both sides, and this behaviour becomes more pronounced at higher temperatures, for example, in Figure 8a,b.

3.2 | Sediment particle size distribution

Figure 9a-d show the changes in the median particle size of the particles deposited in the sand layer at the end of the test in the direction of water infiltration. Figure 9 shows that the median particle size of the particles deposited in the sand layer gradually increases with increasing infiltration distance. At 8.3 cm closer to the inlet, the D_{50} of the particles deposited in the sand layer is extremely small, $\sim 3 \mu\text{m}$. At

an infiltration distance of 13 cm, the particle D_{50} starts to exceed the initial level, and the particle D_{50} deposited in the sand layer is distributed from 15 to 25 μm . Additionally, the higher the temperature is, the larger the D_{50} . This indicates that the process of particle migration in the water-bearing sand layer was blocked, so that the particles that could have migrated did not pass through the pore channels and continued to form a deposit in the sand layer. In addition, Figure 9 shows that the higher the temperature is, the larger the sizes of particles deposited in the sand layer. Temperature has a greater effect on smaller particle sizes than larger ones, and as a result, it is more likely for smaller particles to migrate and spread in all directions at higher temperatures, which is ultimately reflected in the larger median particle size that clogs the sand layer. From Figure 9b,c, it can be seen that the particle size deposited at 25°C is the smallest, and the analysis suggests that too high or too low temperature will be detrimental to the particle deposition in the middle of the sand box.

To more clearly explore the particle deposition process, Figure 10a-c show the particle gradation curves at $x = 8.3 \text{ cm}$. Figure 10 shows that the particles deposited near $x = 8.3 \text{ cm}$ have the

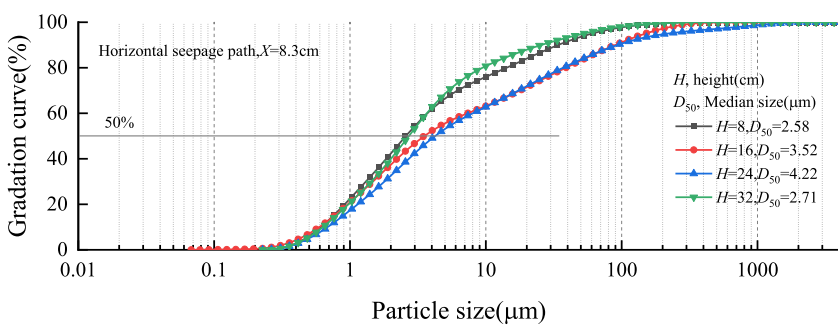
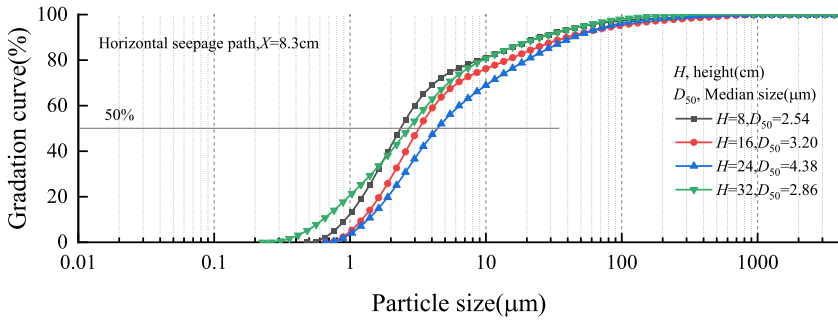
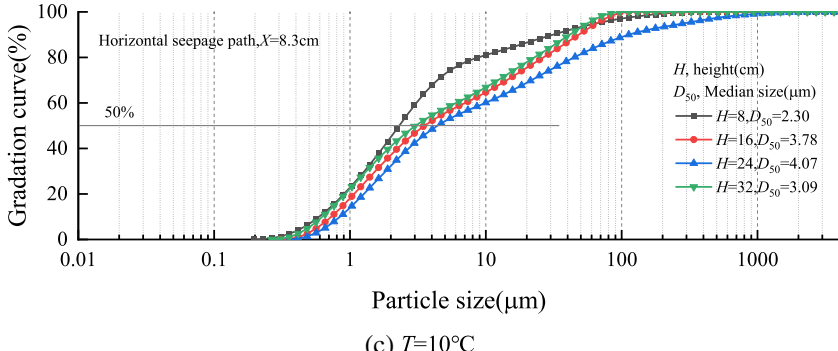
(a) $T=40^\circ\text{C}$ (b) $T=25^\circ\text{C}$ 

FIGURE 10 Particle size distribution of deposited particles at the percolation distance $x = 8.3 \text{ cm}$.

smallest D_{50} at $H = 8$ cm and $H = 32$ cm, and more small particles are deposited in these two layers. This indicates that the migration process of particles in the sand layer is diffusive, and particles with smaller particle sizes are more likely to pass through the pore channels and thus distribute around the sandbox, which is eventually reflected in the reduction in D_{50} . The increase in temperature promotes the diffusion behaviour; for example, D_{50} increases from $2.30 \mu\text{m}$ at 10°C to $2.58 \mu\text{m}$ at 40°C for $H = 8$ cm. In fact, the particles are deposited more in the lower layer of the sandbox than in the upper layer. In the initial percolation section, the particles enter the primary pore channels from all directions and then flow out through the sandbox, and this stage is the diffusion zone. With the continuous entry of suspension, most of the primary pore channels are blocked and particle migration is gradually hindered, and most of them stay in the front end, and this stage is the deposition zone. At low percolation distances small particles take up a larger proportion, thus reducing the median particle size. The temperature change will affect this process,

and the temperature increase or decrease will advance or slow down the deposition zone, which is finally reflected in the different median particle size distribution at each location.

3.3 | Test pressure and permeability coefficient

During the test, the deposition of particles reduces the permeability of the sandbox, and the development of particle deposition and blockage in the sandbox was assessed by observing the change in the permeability coefficient K . The permeability coefficient K was obtained by substituting Darcy's law from the pressure transducer readings and the flow rate through the sandbox:

$$K = \frac{Q\Delta L}{A\Delta H} \quad (2)$$

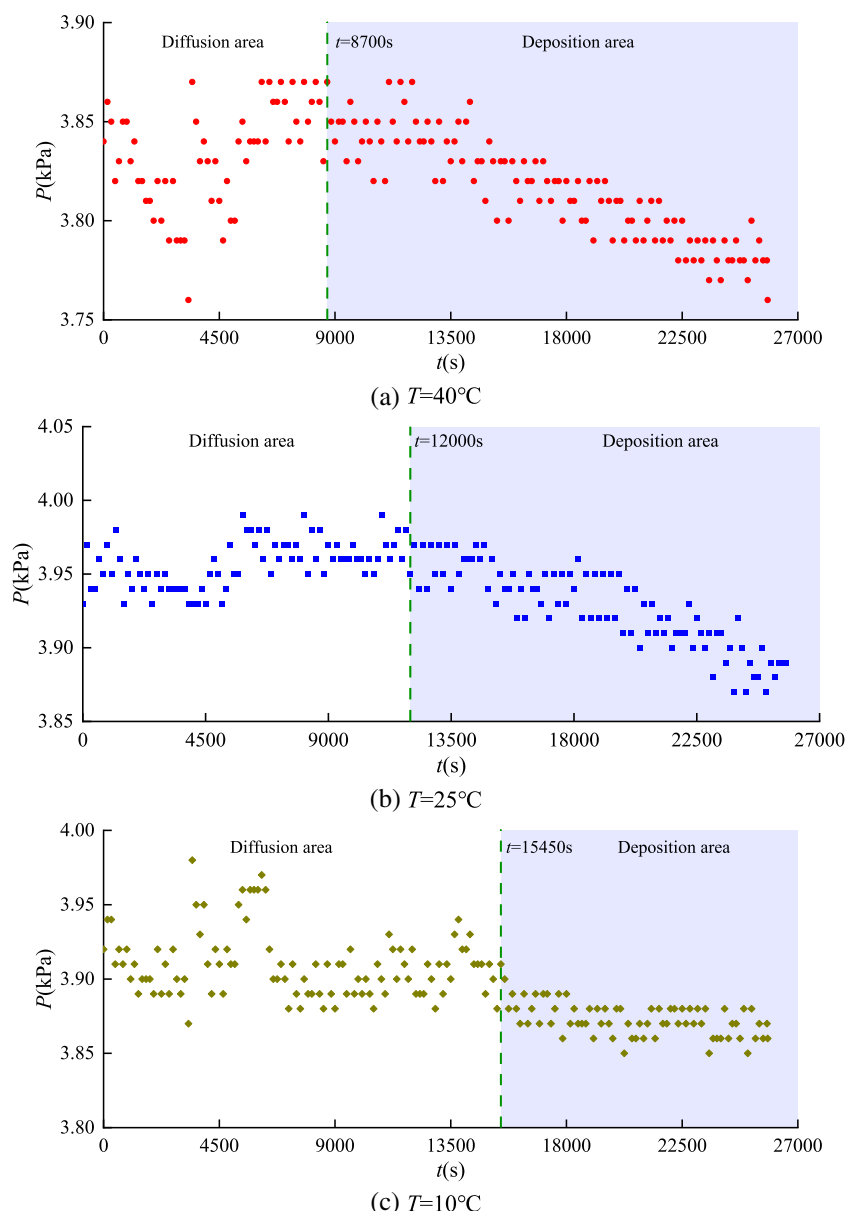


FIGURE 11 Graph of sandbox pressure variation at three test temperatures (pressure monitor #4).

where Q is the flow rate out of the sandbox (m^3/d); ΔL is the distance between the pressure sensors (m); A is the sandbox cross section distance (m^2); and ΔH is the head pressure difference between the pressure sensors (m).

Figure 11 shows the pressure variations monitored during the different tests. Figure 11 shows that the pressure first oscillates continuously back and forth around a fixed value and then decreases steadily. In fact, the migration process of particles in the sand layer is divided into a diffusion zone and a deposition zone. According to the groundwater dynamics, at the beginning of migration, the particles disperse in all directions to fill the pores, including holes that are effective for migration and those that are ineffective for migration, because the inhomogeneous flow of fluid in the porous medium disperses the particles. The pressure P continues to oscillate around a value during this time, and in Figure 11b, the pressure oscillates at $\sim 3.97 \text{ kPa}$ from $t = 0$ to $12\,000 \text{ s}$. As time passes, the porous medium becomes saturated to a certain extent, the pore channels are blocked by dispersed particles, and the particles begin to migrate continuously in the direction of seepage. This process leads to deposition and a steady decrease in pressure. A significant decrease in the permeability coefficient occurs after the particles enter the deposition zone, and the changes in the permeability coefficient after the corresponding time t are listed in Figure 12. In Figure 11b, the pressure decreases from 4 to 3.96 kPa at the end of the test. The change in the permeability coefficient during this process is shown in the figure. Particle deposition causes a decrease in the permeability coefficient in the sand layer, and K decreases from 1.2 to $0.7\text{E}-5 \text{ m/s}$. In addition, the temperature can increase the kinetic energy of the particles, which makes the migration behaviour of the particles in the sand layer occur sooner. In Figure 11, the deposition zone of the test group occurs at 8700 , $12\,000$ and $15\,450 \text{ s}$ at $T = 40^\circ\text{C}$, 25°C , and 10°C .

3.4 | Deposition pictures under microscope

At the end of each set of tests, the samples were dried, removed and placed under a microscope for observation. Figure 13 shows the finely detailed photographs of the particles deposited on the surface of the sand layer. Figure 13a–f show the photographs taken at a migration distance of 10 cm , and (g)–(i) show those taken close to the outlet. From (a) to (f), the photographs clearly show that the particles are deposited in the seams and pits on the surface of the sand during the migration process. As the percolation distance increases, the number of deposited particles increases.

4 | DISCUSSION

This paper discusses research that related to the recharge process of the GWHP system, the independent development of a three-dimensional sandbox seepage test system and the design of a particle migration test based on the Reynolds number. The test results show that temperature has a large influence on the migration-deposition process of particles in wet sand. The Reynolds number is a

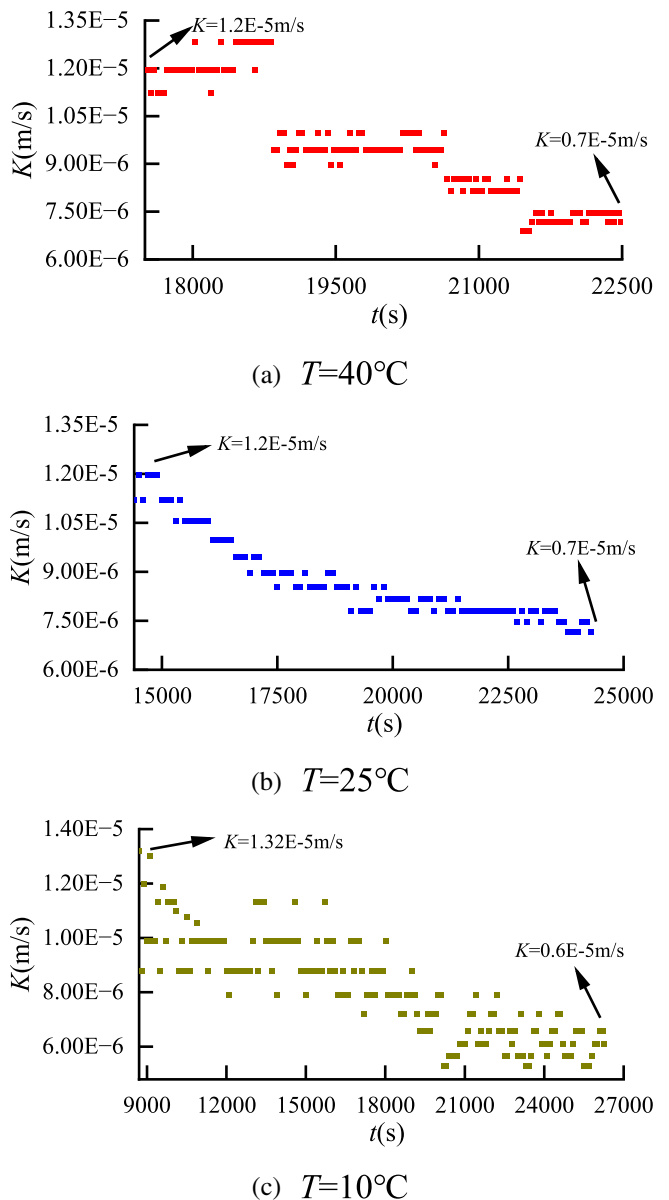


FIGURE 12 The change of permeability coefficient of sand box after the particles enter the deposition zone.

dimensionless number used to characterize the flow state of a fluid. When the Reynolds number is small, the influence of viscous forces on the flow field is greater than the inertial forces, and the fluid undergoes stable laminar flow. Conversely, when the influence of inertial forces on the flow field is greater than the viscous forces, the fluid flow is more unstable. The Reynolds number is defined as:

$$Re = \frac{\rho u L}{\mu} \quad (3)$$

$$\mu = 0.01779 / (1 + 0.03368T + 0.000221T^2) \quad (4)$$

where ρ is the density of the fluid (kg/m^3); u is the fluid velocity (cm/s); L is the characteristic length (m); μ is the viscosity coefficient of water (kg/(m·s)); and T is the Celsius temperature ($^\circ\text{C}$).

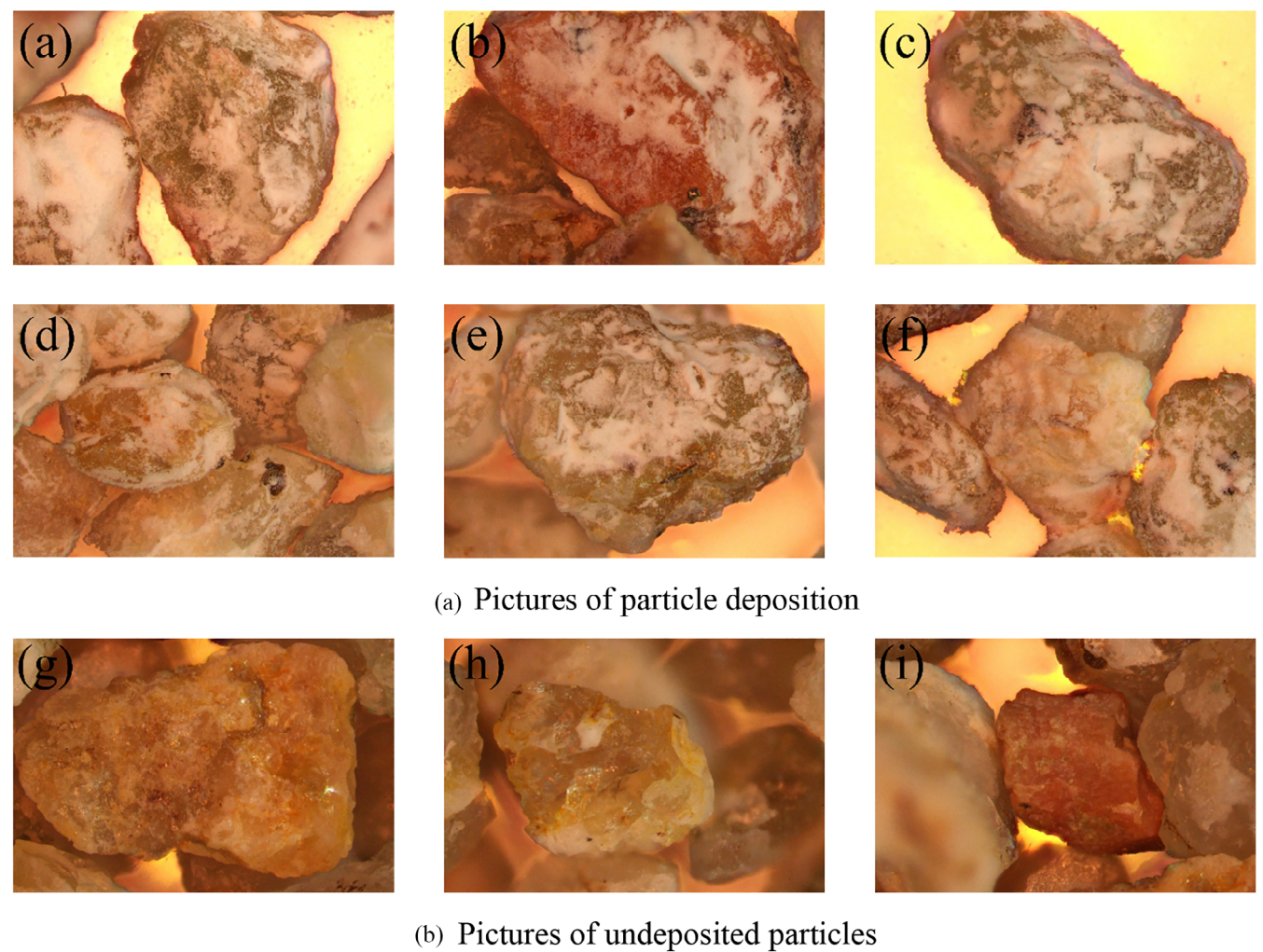


FIGURE 13 Microscopic observation pictures.

TABLE 2 Test Re parameters.

Reynolds number			
u (mm/s)	$T = 10^\circ\text{C}$	$T = 25^\circ\text{C}$	$T = 40^\circ\text{C}$
0.1	0.009	0.013	0.018

The calculation of the Reynolds number in this study is shown in Table 2, which shows that particle migration in porous media is mainly influenced by viscous forces. The maximum Reynolds number under the test conditions is $0.018 \ll 10$, which shows that the water flow is laminar and in accordance with Darcy's law. At higher temperatures, the viscosity of the water decreases, and its resistance to the particles decreases, thus increasing the settling of the particles and depositing more particles in the sand layer. As shown in Figure 8, the deposition of particles in the upper part of the sandbox decreases significantly with increasing temperature. In Figure 8b for $H = 32\text{ cm}$ and in Figure 8c for $H = 16, 24$, and 32 cm , the mass percentage R of particles to sand does not exceed 0.05%. The increase in temperature also promotes the increase in particle kinetic energy, which leads to an

increase in the frequency of collisions between particles and natural sand so that more particles are captured by the natural sand medium, which is eventually reflected in the increase in deposition. In addition, the deposition coefficient and longitudinal dispersion coefficient of suspended particles increase with increasing temperature, which leads to a wider distribution range of suspended particles in the sandbox. Additionally, due to the increase in kinetic energy of the particles, the time spent in the process of diffusion in the sand layer is shortened, that is, the diffusion zone ends sooner, as shown in Figure 11, where the deposition zone of the particles advances by 6750 s under 40°C test conditions compared to 10°C . As the particles enter the deposition phase sooner, the final deposition volume increases. In addition, Figure 9 shows that the higher the temperature is, the larger the sizes of the particles deposited in the sand layer because the smaller particles are more sensitive to temperature and migrate faster with the flowing water.

In summary, the temperature increase causes more particles to be deposited in the sand layer and accelerates the uneven flow of particles in the sand layer. The particles spread in the non-direction of percolation, and the higher the temperature is, the more obvious this

diffusion behaviour is, which eventually broadens the distribution range of the suspended particles in the sandbox. The increase in temperature also promotes the percolation of small particles and causes the diffusion zone to end sooner, thus extending the deposition zone and increasing the number of particles captured at the surface and in the pore channels of the sand layer.

5 | CONCLUSION

This article explores the effect of temperature on the transport process of suspended particles in porous media through a three-dimensional percolation sandbox test system that was developed in this laboratory and verifies the rationality of the test by microscopic observations. The following conclusions are drawn:

1. Temperature changes can significantly affect the transport process of suspended particles in layers of wet sand. An increase in temperature causes the deposition of more particles in the sand layer, even though the mass percentage of particles to sand increases.
2. A temperature increase accelerates the uneven flow of particles in the sand layer, and the particles spread in the non-direction of percolation. The higher the temperature is, the more obvious this diffusion behaviour is, which eventually broadens the distribution range of suspended particles in the sandbox. A temperature increase also promotes the percolation of smaller particles, as they are more sensitive to temperature changes, and the median particle size D_{50} deposited in the sand layer increases.
3. The migration of particles in the layer of wet sand is complex, and there are diffusion zones and deposition zones through the test. The temperature increase causes the diffusion zone to end sooner, thus extending the deposition zone and increasing the number of particles captured on the surface and in the pore channels of the sand layer.

The experimental study found that particles form clogs not far from migration in the sand layer, and the increase in the filtration level not far from the radial direction of the wellbore retards particle clogging. However, it is necessary to confirm this conclusion by further tests. Additionally, it is possible to reduce the probability of forming clogs by appropriately reducing the temperature of the backflow water to reduce the diffusion of particles in the radial direction of the wellbore.

To better understand the migration of suspended particles in aquifers during GWHP operations, field tests and monitoring should be conducted in conjunction with actual projects. This will be the focus of future research along with the study of blockages of water sources during recharge by heat pumps under actual operating conditions and its impact on the formation environment.

ACKNOWLEDGEMENTS

This research was supported by the National Natural Science Foundation of China (Grant No. 41702254), the Natural Science Foundation

of Hubei Province (Grant No. 2022CFB248), Educational Commission of Hubei Province of China (T2020005), the Young Top-notch Talent Cultivation Program of Hubei Province, and Research Project of Hubei Provincial Department of Education (B2021037).

DATA AVAILABILITY STATEMENT

The data that support the findings of this study are available from the corresponding author upon reasonable request.

ORCID

Xianze Cui  <https://orcid.org/0000-0003-4120-2971>

REFERENCES

- Ahfir, N. D., Hua, Q. W., Benamar, A., Alem, A., Massei, N., & Dupont, J. P. (2007). Transport and deposition of suspended particles in saturated porous media: Hydrodynamic effect. *Hydrogeology Journal*, 15(4), 659–668.
- Ahmadi, M. H., Ahmadi, M. A., Sadaghiani, M. S., Ghazvini, M., Shahriar, S., & Nazari, M. A. (2018). Ground source heat pump carbon emissions and ground-source heat pump systems for heating and cooling of buildings: A review. *Environmental Progress & Sustainable Energy*, 37(4), 1241–1265.
- Alem, A., Elkawafi, A., Ahfir, N. D., & Wang, H. Q. (2013). Filtration of kaolinite particles in a saturated porous medium: Hydrodynamic effects. *Hydrogeology Journal*, 21(3), 573–586.
- Bai, B., Long, F., Rao, D., & Xu, T. (2016). The effect of temperature on the seepage transport of suspended particles in a porous medium. *Hydrological Processes*, 31(2), 382–393.
- Bai, B., Nie, Q., Wu, H., & Hou, J. (2021). The attachment-detachment mechanism of ionic/nanoscale/microscale substances on quartz sand in water. *Powder Technology*, 394(6), 1158–1168.
- Bai, B., Zhang, J., Liu, L., & Ji, Y. (2020). The deposition characteristics of coupled lead ions and suspended silicon powders along the migration distance in water seepage. *Transport in Porous Media*, 2, 1–18.
- Bennacer, L., Ahfir, N. D., Bouanani, A., Alem, A., & Wang, H. (2013). Suspended particles transport and deposition in saturated granular porous medium: Particle size effects. *Transport in Porous Media*, 100(3), 377–392.
- Bing, B. A., Qnb, C., Yz, A., Xw, A., & Wei, H. D. (2021). Cotransport of heavy metals and SiO_2 particles at different temperatures by seepage. *Journal of Hydrology*, 597, 125771.
- Blum, P., Campillo, G., & Kölbel, T. (2011). Techno-economic and spatial analysis of vertical ground source heat pump systems in Germany. *Energy*, 36(5), 3002–3011.
- Chrysikopoulos, C. V., & Aravantinou, A. F. (2014). Virus attachment onto quartz sand: Role of grain size and temperature. *Journal of Environmental Chemical Engineering*, 2(2), 796–801.
- Cui, X., Fan, Y., & Wang, H. (2019). Ground environment characteristics during the operation of GWHP considering the particle deposition effect. *Energy and Buildings*, 206, 109593.
- Cui, X., Fan, Y., Wang, H., & Huang, S. (2019). Effects of temperature on the transport of suspended particles through sand layer during groundwater recharge. *Water, Air, and Soil Pollution*, 230(10), 251.1–251.13.
- Dallmann, J., Phillips, C. B., Teitelbaum, Y., Sund, N., & Packman, A. I. (2020). Impacts of suspended clay particle deposition on sand-bed morphodynamics. *Water Resources Research*, 56.
- Dong, S., Xia, J., Sheng, L., Wang, W., & Gao, B. (2021). Transport characteristics of fragmental polyethylene glycol terephthalate (pet) microplastics in porous media under various chemical conditions. *Chemosphere*, 276, 130214.

- García-Gil, A., Epting, J., Ayora, C., Garrido, E. E., Vázquez-Suñ, É., Huggenberger, P., & Cristina Gimenez, A. (2016). A reactive transport model for the quantification of risks induced by groundwater heat pump systems in urban aquifers. *Journal of Hydrology*, 542, 719–730.
- Gjengedal, S., Ramstad, R. K., Hilmo, B. O., & Frengstad, B. S. (2020). Fouling and clogging surveillance in open loop GSHP systems. *Bulletin of Engineering Geology and the Environment*, 79(1), 69–82.
- Jiang, Y., Yin, X., Xi, X., Guan, D., & Wang, N. (2021). Effect of surfactants on the transport of polyethylene and polypropylene microplastics in porous media. *Water Research*, 196, 117016.
- Kim, H. N., & Walker, S. L. (2009). Escherichia coli transport in porous media: Influence of cell strain, solution chemistry, and temperature. *Colloids & Surfaces B Biointerfaces*, 71(1), 160–167.
- Li, C., Dai, C., & Lei, H. (2016). Deposition and transport properties of suspended particles in heated porous media. *Journal of Chemical Engineering*, 67(4), 7.
- Liu, Q., Cui, X., & Zhang, C. (2015). Experimental study on the detachment characteristics of deposited particles in porous media. *Chinese Journal of Geotechnical Engineering*, 37(4).
- Lumbangaol, C., Ganzer, L., Mukherjee, S., & Hakan, A. (2021). Investigation of clogging in porous media induced by microorganisms using a microfluidic application. *Environmental Science: Water Research & Technology*, 7, 441–454.
- Mauclaire, L., Schuermann, A., & Mermilliod-Blondin, F. (2006). Influence of hydraulic conductivity on communities of microorganisms and invertebrates in porous media: A case study in drinking water slow sand filters. *Aquatic Sciences*, 68(1), 100–108.
- Mek, A., Jsw, A., Jn, B., Jplka, C., Sk, A., & Djwa, D. (2020). Experimental study of pH effect on uranium (VI) particle formation and transport through quartz sand in alkaline 0.1M sodium chloride solutions. *Colloids and Surfaces A: Physicochemical and Engineering Aspects*, 592, 124375.
- Nie, Q., Li, H., Yang, H., Ni, T., & Jiang, S. (2021). The promotion/inhibition of the seepage transport of copper ions by suspension-colloidal particles with wide size gradation. *Geofluids*, 3, 1–12.
- Pan, D., Tang, H., & Liu, J. (2021). Analysis of unsaturated seepage blockage in groundwater source heat pump recharge. *Journal of Rock Mechanics and Engineering*, 40(4), 9.
- Rosenbrand, E., Haugwitz, C., Jacobsen, P., Kjoller, C., & Fabricius, I. L. (2014). The effect of hot water injection on sandstone permeability. *Geothermics*, 50, 155–166.
- Sarbu, I., & Sebarchievici, C. (2014). General review of ground-source heat pump systems for heating and cooling of buildings. *Energy & Buildings*, 70, 441–454.
- Sasidharan, S., Torkzaban, S., Bradford, S. A., Dillon, P. J., & Cook, P. G. (2014). Coupled effects of hydrodynamic and solution chemistry on long-term nanoparticle transport and deposition in saturated porous media. *Colloids & Surfaces A Physicochemical & Engineering Aspects*, 457, 169–179.
- Seifert, D., & Engesgaard, P. (2012). Sand box experiments with bioclogging of porous media: Hydraulic conductivity reductions. *Journal of Contaminant Hydrology*, 136–137, 1–9.
- Shabani, A., Kalantariasl, A., Parvazdavani, M., & Abbasi, S. (2019). Geochemical and hydrodynamic modelling of permeability impairment due to composite scale formation in porous media. *Journal of Petroleum Science & Engineering*, 176, 1071–1081.
- Shaniv, D., Dror, I., & Berkowitz, B. (2021). Effects of particle size and surface chemistry on plastic nanoparticle transport in saturated natural porous media. *Chemosphere*, 262, 127854.
- Tao, G., Wu, X., Xiao, H., Chen, Q., & Cai, J. (2019). A unified fractal model for permeability coefficient of unsaturated soil. *Fractals*, 27(1), 1940012.
- Wang, Y., Xu, L., Chen, H., & Zhang, M. (2022). Retention and transport behavior of microplastic particles in water-saturated porous media. *Science of the Total Environment*, 808, 152154.
- Won, J., Choo, H., & Burns, S. E. (2020). Impact of solution chemistry on deposition and breakthrough behaviors of kaolinite in silica sand. *Journal of Geotechnical and Geoenvironmental Engineering*, 146(1), 4019123.1–4019123.10.
- Xue, C., Wang, Y., & Liu, G. (2019). Effect of temperature and pH on the osmotic migration of suspended particles in porous media. *Journal of Geotechnical Engineering*, 41(11), 8.
- You, Z., Bedrikovetsky, P., Badalyan, A., & Hand, M. (2015). Particle mobilization in porous media: Temperature effects on competing electrostatic and drag forces. *Geophysical Research Letters*, 42(8), 2852–2860.

How to cite this article: Cui, X., Li, J., Yang, G., Fei, W., Ding, S., & Fan, Y. (2023). Spatial migration and distribution of suspended particles in saturated sand layer under the impact of temperature. *Hydrological Processes*, 37(2), e14833. <https://doi.org/10.1002/hyp.14833>